KeAi
CHINESE ROOTS
GLOBAL IMPACT

Available online at www.sciencedirect.com

ScienceDirect

Advances in Climate Change Research 11 (2020) 360–369

www.keaipublishing.com/en/journals/accr/

A shallow ice core from East Greenland showing a reduction in black carbon during 1990–2016

DU Zhi-Heng[a,b], XIAO Cun-De[c,*], DOU Ting-Feng[d], LI Chuan-Jin[a], DING Ming-Hu[e], Sangeeta SHARMA[f], MA Xiang-Yu[a], WANG Shi-Meng[a], ZHANG Wang-Bin[g]

[a] *State Key Laboratory of Cryospheric Science, Northwest Institute of Eco-Environment and Resources, Chinese Academy of Sciences, Lanzhou, 730000, China*
[b] *Southern Marine Science and Engineering Guangdong Laboratory, Guangzhou, 511458, China*
[c] *State Key Laboratory of Earth Surface Processes and Resource Ecology, Beijing Normal University, Beijing, 100875, China*
[d] *University of Chinese Academy of Science, Beijing, 100049, China*
[e] *State Key Laboratory of Severe Weather, Chinese Academy of Meteorological Sciences, Beijing, 100081, China*
[f] *Climate Research Division, Environment and Climate Change Canada, Toronto, M3H 5T4, Canada*
[g] *School of Geographic and Oceanographic Sciences, Nanjing University, Nanjing, 210023, China*

Received 3 March 2020; revised 9 June 2020; accepted 27 November 2020
Available online 11 December 2020

Abstract

This study reports on the measurements of ion and refractory black carbon (rBC) concentrations in a shallow (10.96 m) ice core sample which was drilled from the field site of the East Greenland Ice Core Project (EGRIP) in July, 2016. The results provide a recent record of rBC deposition in the East Greenland ice sheet from 1990 to 2016. The annual variability in oxygen ($\delta^{18}O$) and hydrogen (δD) isotopic compositions indicated that notably warm events occurred since 2008. Peaks in rBC occurred during summer seasons, which may be attributed to the burning of biomass in boreal summer. The rBC record and analysis of historical air trajectories using the HYSPLIT model indicated that anthropogenic BC emissions from Russia, North America and Europe contributed to the majority of rBC deposition in the Greenland region, and a reduction in anthropogenic BC consumption in these areas played a dominant role in the decrease in BC concentrations since 2000. This record also suggests that the emissions from the East Asian region (China) contributed very little to the recorded BC concentrations in East Greenland ice core. The model results indicated that radiative forcing due to BC had decreased significantly since 1990, and had remained below 0.02 W m^{-2} since 2000.

Keywords: East Greenland; Ice core; Black carbon; Seasonal variability; Potential emission sources

1. Introduction

Black carbon (BC) is the absorbing component of soot and originates from the combustion of biomass and fossil fuels (Winiger et al., 2019). BC can affect the albedo of snow and ice when deposited on the ground surface, and the radiative forcing (RF) of BC in snow is an important factor enhancing the melting of glacier and ice sheets, particularly in Greenland (Xu et al., 2009; Li et al., 2016; Li and Flanner, 2018; Winiger et al., 2019). BC has been recognized as an important contributor to anthropogenic climate change since the 1980s (Warren, 2019). Therefore, various studies have focussed on the effects of BC in snow on the climate (Skiles et al., 2018). However, the quantitative impact of BC on the ablation of glaciers remains highly uncertain due to the high spatial and content variabilities of BC (Mcconnell et al., 2007; IPCC, 2013; Mori et al., 2019).

Studies on the deposition of BC and the resulting contribution to the melting of snow and ice over the Pan-Arctic

* Corresponding author.
E-mail address: cdxiao@bnu.edu.cn (XIAO C.-D.).
Peer review under responsibility of National Climate Center (China Meteorological Administration).

https://doi.org/10.1016/j.accre.2020.11.009

region are relatively mature (Flanner et al., 2007; Dou et al., 2012; Lin et al., 2014; Polashenski et al., 2015). Previous studies have suggested that the RF of BC deposition over the Arctic could be as much as 0.23 W m^{-2} during years with high emissions, far exceeding the global mean of 0.05 W m^{-2} (Flanner et al., 2007). Model simulations have indicated that the RF of organic aerosols deposited in snow/ice ranges from +0.0011 W m^{-2} to +0.0031 W m^{-2}, which can account for 24% of the forcing resulting from BC in snow and ice (Lin et al., 2014). However, model simulations are not available for the Greenland region due to a lack of continuous field measurements (Hirdman et al., 2010; Dou et al., 2012). Greenland ice core data can to some extent compensate for this lack of modelled data, and ice core data are also suitable for use in the investigation of long-term changes in emissions of BC within the Northern Hemisphere (Mcconnell et al., 2007). Ice cores contain detailed paleo-climatic environment information, including data for impurities, short-lived aerosols and BC, which can provide a unique historical record of past aerosol loads. Therefore, the reconstruction of historical BC from ice core archives can help to calculate historical emissions and can also provide additional constraints on the climatic effect of BC (Mcconnell et al., 2007; Ming et al., 2009; Xu et al., 2009; Bisiaux et al., 2012).

Ice cores drilled at high-altitude European Alpine sites have since the mid-20th century highlighted a pronounced increase in BC concentrations (Legrand et al., 2007; Thevenon et al., 2009). Several ice-core records of refractory BC (rBC) deposition in the Arctic are available from Greenland and Svalbard (Koch et al., 2007; Mcconnell et al., 2007; Lee et al., 2013; Ruppel et al., 2014; Zennaro et al., 2014; Zdanowicz, 2018; Osmont et al., 2018; Sigl et al., 2018), which have shown that historical BC records can be attributed to anthropogenic emissions and the transport of BC to the Pan-Arctic region. However, the majority of these ice cores were dated before 2000, resulting in a lack of comprehensive understanding of BC deposition after 2000. The present study used BC records reconstructed from a shallow ice core (10.96 m) near the East Greenland Ice core Project (EGRIP) research site (75°37′N, 35°59′W, 2702 m above sea level (a.s.l)). The reconstructed BC records were used to investigate BC deposition in East Greenland over the last three decades, and to be compared with those over other Arctic regions. The present study conducted a preliminary investigation on the possible reasons for the spatial differences in BC deposition within the Pan-Arctic region.

2. Methods

2.1. Ice core collection and treatment

A shallow ice core sample (depth 10.96 m, diameter 7.0 cm) was drilled at the EGRIP research site in July, 2016 (Fig. 1). The shallow ice core samples were maintained in a frozen condition and shipped to the State Key Laboratory of Cryospheric Science (SKLCS) in Lanzhou. The thicknesses of annual layers were determined from a previous ice core collected at the EGRIP

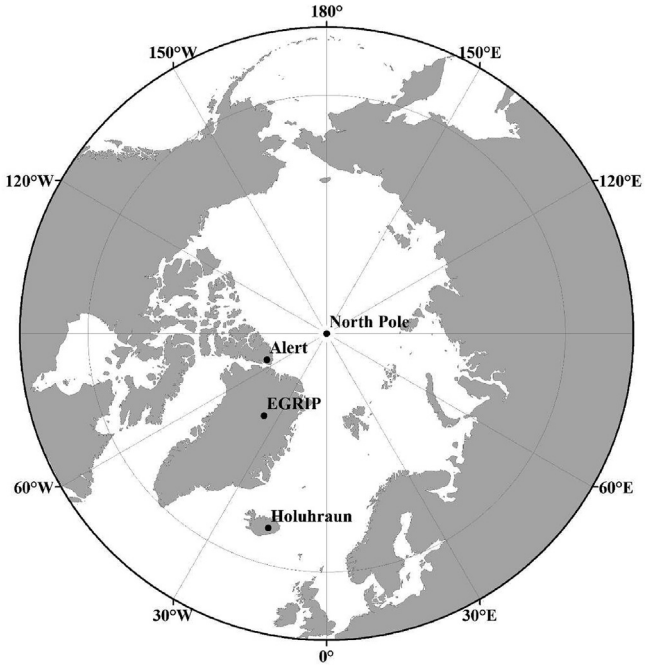

Fig. 1. Map showing the research site of the East Greenland Ice core Project (EGRIP) where a shallow ice core was collected, along with other reference locations such as the Alert station, the North Pole and the site of the Holuhraun volcano eruption.

site, which showed an ice accumulation rate of about 0.11 m per year (ice equivalent) (Vallelonga et al., 2014). During the processing of ice core samples, the samples were first cut at intervals of 4–5 cm to ensure the availability of a mean of 8–9 subsamples per year for the determination of the temporal resolutions of major ions, rBC, and stable oxygen ($\delta^{18}O$) and hydrogen (δD) isotopes. The outermost 5 mm layer of each core section was then removed using a lathe to eliminate contamination that may have occurred due to drilling, transport, and storage processes. This outer layer was removed using a ceramic blade cleaned with ultrapure deionized (DI) water, with the process repeated three times. The final processed inner core section was placed into an acid-cleaned polypropylene (PP) bottle (Thermo Fisher Scientific). The above processes were performed in a Class 100 laminar cleaning flow bench (−12 °C). The second layer of each ice section was wiped free of contamination using a pre-cleaned ceramic blade, following which the inner section was melted at 20 °C and the resulting melt water was transferred into a 1.5 ml glass bottle for analyses of $\delta^{18}O$ and δD isotopes. More details on the research method can be found in Du et al. (2020).

2.2. Quantification

The cleaned ice samples were melted at room temperature (~20 °C), following which measurements were conducted using a Picarro L2130-i Cavity Ring-Down Spectrometer. $\delta^{18}O$ and δD measurements were calibrated against the Vienna Standard Mean Ocean Water (VSMOW). Analytical precisions of 0.1‰ and 0.5‰ were adopted for $\delta^{18}O$ and δD,

respectively. Ion analyses (Na^+ and SO_4^{2-}) were performed on an ion chromatograph (Dionex ISC3000, Thermo Scientific, USA). Approximately 2 ml of sample was injected, following which isocratic and gradient analyses were conducted for determination of cations and anions, respectively (Du et al., 2018). The errors originating from replicate sample measurements were within 5% of standard samples. The detection limits, defined as three times the standard deviation of the baseline noise, were approximately 1 ng g^{-1} for all major ions. The non-sea-salt (nss) fractions for SO_4^{2-} were calculated by first assuming that all Na^+ originates from sea salt (ss). The non-sea-salt fraction [nss SO_4^{2-}] = [SO_4^{2-}]−([SO_4^{2-}]/[Na^+])$_{sea}$ × [Na^+] as sea salt aerosol (SO_4^{2-}) is primarily emitted from the open ocean (the bulk sea water ion weight ratio of [SO_4^{2-}]/[Na^+] = 0.252) (Kaufmann et al., 2010).

rBC was analyzed using a Single Particle Soot Photometer (SP2) coupled with an ultrasonic nebulization system (CETAC3tan Plateau Research, Chinese Academy of Sciences. rBC was defined based on the mass of the specific absorbing components of individual aerosol particles, and was measured using a SP2 (Schwarz et al., 2010). The SP2 was used with laser-induced incandescence to measure the mass of rBC in individual particles (Schwarz et al., 2006). The rBC particles were directed by a jet stream through a Nd:YAG laser. The intensity of the intracavity light (~10^6 W cm^{-2}) was sufficiently strong to vaporize light absorbing particles (Stephens et al., 2003; Baumgardner et al., 2007; Wang et al., 2015). That incandescence signal, detected by photomultiplier tube detectors, can be converted to an rBC mass. This method has been applied to ice core samples in previous studies (Mcconnell et al., 2007; Bisiaux et al., 2012; Wang et al., 2015). The rBC samples were ultrasonically agitated for 15 min prior to analysis. Detailed information of the SP2 analytical process and calibration procedures have been described in Wang et al. (2015).

3. Results and discussion

3.1. Dating of the ice core

Since the measured $\delta^{18}O$ and δD values of the EGRIP shallow core were highly correlated with each other (r^2 = 0.98), it is evident that the isotopes showed similar behavior during the fractionation processes. The $\delta^{18}O$ and δD values showed distinct seasonal variation, with high and low values during summer and winter, respectively (Fig. 2). Therefore, the shallow core could be dated by counting annual layers using seasonal variations in $\delta^{18}O$ and δD (Fig. 2). As shown in Fig. 2, each annual layer represents two parts, consistent with different snow deposition rates under winter and summer conditions. Vallelonga et al. (2014) dated the topmost annual layer of a shallow ice core using $\delta^{18}O$ values as 2016, with dating uncertainty estimated to be less than ± 1 year over a period extending from 1990 to 2016. The study by Vallelonga et al. (2014) used a high temporal resolution of $\delta^{18}O$ values, with 8–9 subsamples per year.

The mean $\delta^{18}O$ and δD values of the EGRIP shallow ice core in 1990–2016 were −37.1‰ ± 2.0‰ and −286.7‰ ± 13.8‰, respectively. The $\delta^{18}O$ and δD measurements showed considerable fluctuation during 1990–2016, including a decreasing trend beginning in 1992, with the lowest $\delta^{18}O$ and δD values observed at 1996 (Fig. 2). Steady warming then occurred until 2004, with high and significantly oscillating $\delta^{18}O$ and δ D values as the record entered the 21st century, indicating that cold and warm events had become more extreme. The warmest years in the record were 2003, 2008, 2010, 2012 and 2016, with all occurring in the 21st century (2000–2016), whereas the highest $\delta^{18}O$ value occurred in 2012 followed by 2008, with values of −29.3‰ and −31.0‰, respectively. The extent of Arctic sea ice observed on 13 September, 2012 was the lowest on record since November, 1978 (Parkinson and Comiso, 2013). The record obtained from the EGRIP shallow ice core was divided into three 10-year periods of 1990–1999, 2000–2009, and 2010–2016, with the mean $\delta^{18}O$ value for each period being −37.96‰ (std. dev. ± 1.48), −36.42‰ (std. dev. ± 1.95), and −36.62‰ (std. dev. ± 2.23), respectively. The 10-year mean during 2000–2009 was slightly higher compared with that during 2010–2016 because of extreme high and low temperatures occurring during 2010–2016. This result is further evidence of a significant increase in temperature during the 21st century (Karl et al., 2015). The abnormally low D-excess values in the EGRIP shallow ice core record can be explained by the effects of re-evaporation of snow crystals during precipitation or low kinetic effects (Steen-Larsen et al., 2011). As can be seen in Fig. 2, the record shows lower D-excess values for 2007, 2010, 2011, and 2015, suggesting that water vapor originating from the Arctic ocean may have a significant effect in decreasing temperatures.

3.2. rBC record

The rBC concentrations varied between 0.03 and 2.55 ng g^{-1}, with the maximum value recorded during the late 1990s, and a declining trend evident since 2000. Prior to 2000, the mean rBC concentration and flux in this shallow ice core were 0.57 ng g^{-1} and 3.0 ng cm^{-2} per year, respectively, approximately twice the mean value after 2000 of 0.29 ng g^{-1}. In contrast, the mean rBC concentration measured in the Greenland D4 ice core was 2.6 ng g^{-1} during 1990–2000 (Mcconnell et al., 2007), considerably higher than that of the EGRIP shallow ice core. After removing the nss [SO_4^{2-}] data representing the eruption of the Holuhraun Volcano (2014–2015), the mean nss SO_4^{2-} concentrations before and after 2000 were 120.22 ng g^{-1} and 50.23 ng g^{-1}, respectively. Besides, for the contribution of the volcanic source, the EGRIP shallow ice core did not record a remarkable increase in rBC concentration after the eruption.

The record obtained from the EGRIP shallow ice core record showed a clear seasonal rBC cycle (Fig. 3). Winter values were generally lower and ranged from 0.04–0.35 ng g^{-1} with a mean of 0.29 ng g^{-1}. In contrast, summer concentrations ranged from 0.09–1.74 ng g^{-1} with a mean of 0.71 ng g^{-1},

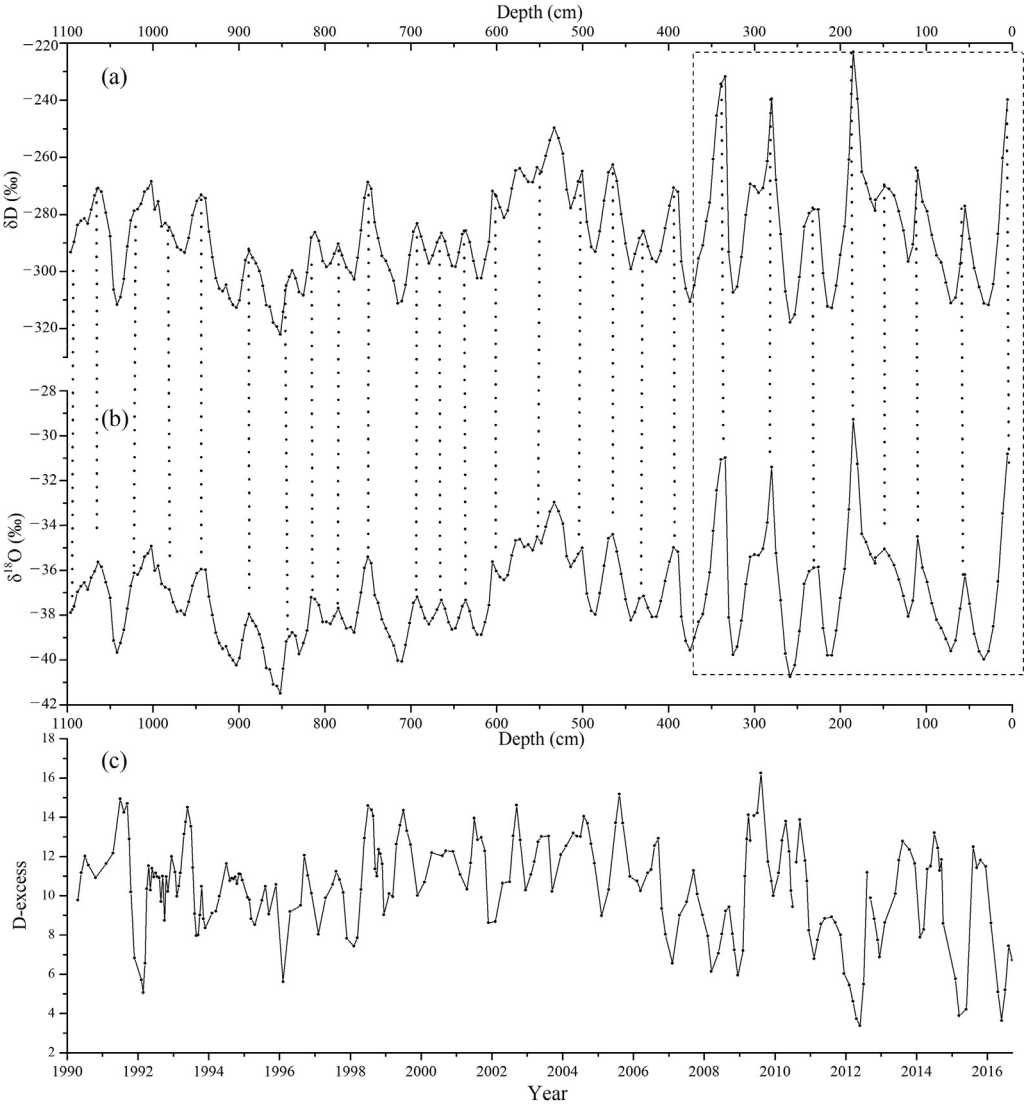

Fig. 2. The δD values (a), $\delta^{18}O$ values (b), and D-excess (c) corresponding to depth and age of a shallow ice core collected from East Greenland Ice core Project (EGRIP) (The dotted box indicated that the frequencies of maximum (minimum) δD and $\delta^{18}O$ values have increasing trend since 2008).

which were identified by higher values of $\delta^{18}O$ (Fig. 3). The seasonal cycle evident in the EGRIP shallow ice core record is different from that observed by Sharma et al. (2013) for a shallow ice core collected from the Arctic Alert station, where BC concentrations were high in winter/spring and low in summer.

Although the mean rBC in summer was higher than that in winter, as shown in Fig. 3, the rBC peaks also occurred in winter. A recent study showed that the sources of elemental carbon (EC) at four Arctic sites were dominated by emissions originating from combustion of fossil fuels during winter and by burning of biomass during in summer (Winiger et al., 2019). Modeling studies and observations have demonstrated that boreal forest fires and biomass burning are the dominant sources of BC in the Arctic during summer (Schneidemesser et al., 2009; Stohl et al., 2013; Mouteva et al., 2015). For example, biomass burning contributed 39% ± 10% of the annual mean BC of the circum-Arctic region (Winiger et al., 2019). Therefore, forest fires and biomass burning may be considered as an additional source of BC which resulted in summer peaks in rBC within the record from the EGRIP shallow ice core. In addition, the difference in observed seasonal patterns in rBC between the EGRIP shallow ice core and observations by Sharma et al. (2013) may be explained by differences in atmospheric boundary layers, as the elevation of the EGRIP shallow ice core was 2702 m, whereas that of the shallow ice core in Sharma et al. (2013) was 210 m.

The median RFs of BC in early summer (June and July) in Greenland prior to 1850, during 1850–1951, and after 1951 were ~0.20 W m^{-2}, ~0.38 W m^{-2}, and ~0.22 W m^{-2}, respectively (Mcconnell et al., 2007). The Matlab column version of the Snow, Ice, and Aerosol Radiative (SNICAR) model was used to simulate the effects of BC on surface ice albedo (Flanner et al., 2007). The modelling assumed a constant snow grain radius of 100 μm with no significant aging.

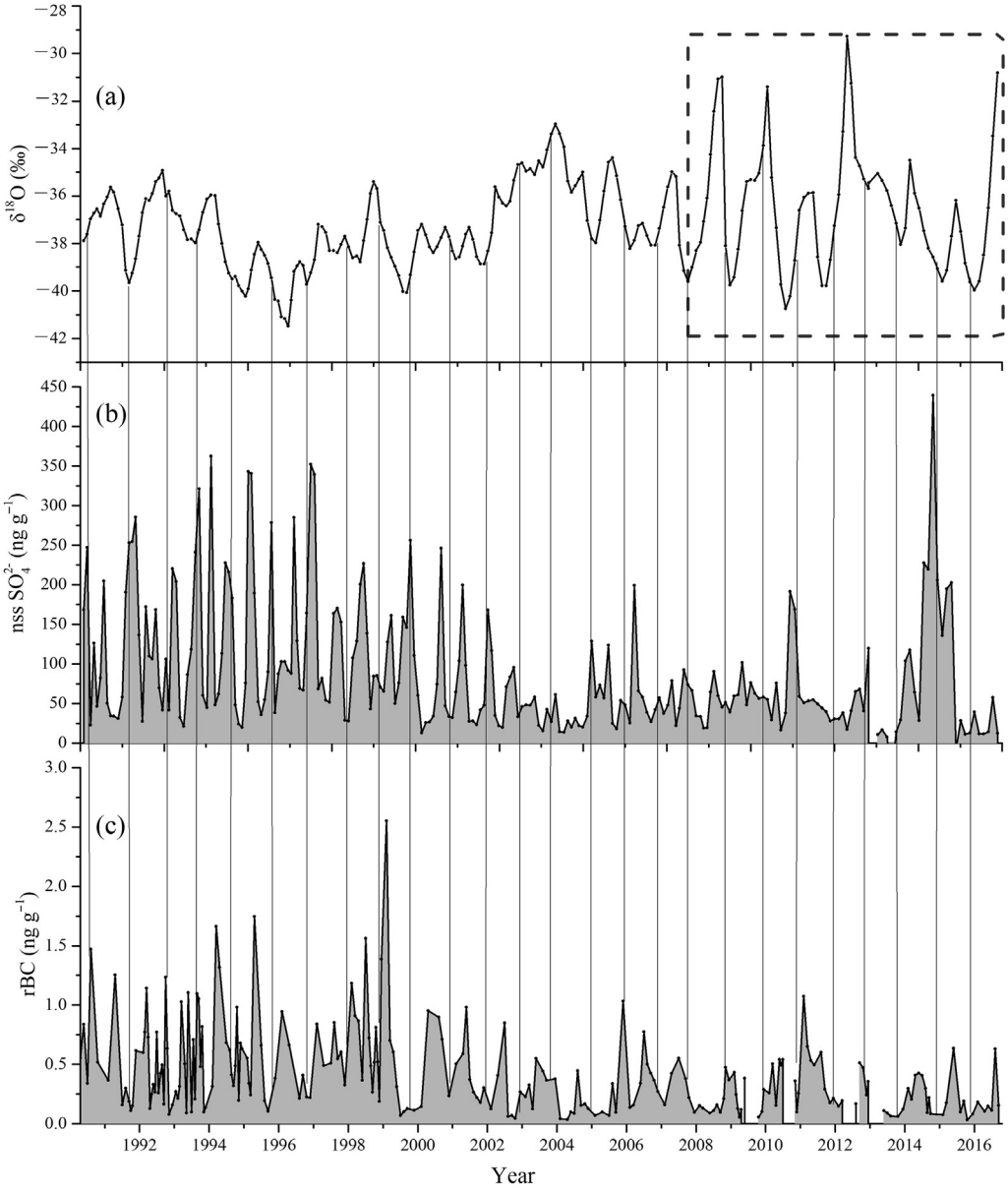

Fig. 3. East Greenland Ice core Project (EGRIP) shallow ice core records of $\delta^{18}O$ (a), non-sea-salt (nss) [SO_4^{2-}] (b), and versus variations in refractory black carbon (rBC) (c) during 1990−2016 (The vertical lines represent the winter seasons whereas the dotted box indicates significant warming during 2008−2016).

The annual mean RF was evaluated by rBC with National Centers for Environment Prediction (NCEP) downwelling surface solar radiation. As shown in Fig. 4, the RF due to BC deposition showed a consistent declining trend during 2000−2016. In particular, the annual mean surface RF values prior to and after 2000 were 0.029 W m^{-2} and 0.013 W m^{-2}, respectively.

3.3. Regions of potential emission sources

The increase in fossil fuel emissions in China since 2000 has not resulted in a concurrent increase in rBC in the EGRIP shallow ice core. Studies based on ground observations of aerosol BC over the Alaskan Arctic (Barrow station), Canadian Arctic (Alert station), and Svalbard (Zepplin station) have shown a decline in winter BC concentrations by 40% between 1990 and 2009, which is the most significant change in BC since the early 1990s (Sharma et al., 2013). Observations of carbonaceous species in snow at the Summit station has shown clear seasonal variations, with higher spring or summer concentrations (Hagler et al., 2007; Stohl et al., 2013). This seasonal deposition most likely results from smoke plumes, including from forest or grassland fires, which are transported to the Arctic by the prevailing summer winds (Stohl, 2006; Paris et al., 2009; Warneke et al., 2009; Zennaro et al., 2014). Further analysis showed a discrepancy in BC values between the Summit station and the Alert station, indicating that BC aerosols are transported from the polluted boundary layer to higher altitudes with efficient upward transport occurring during summer, mainly driven by thermal convection and

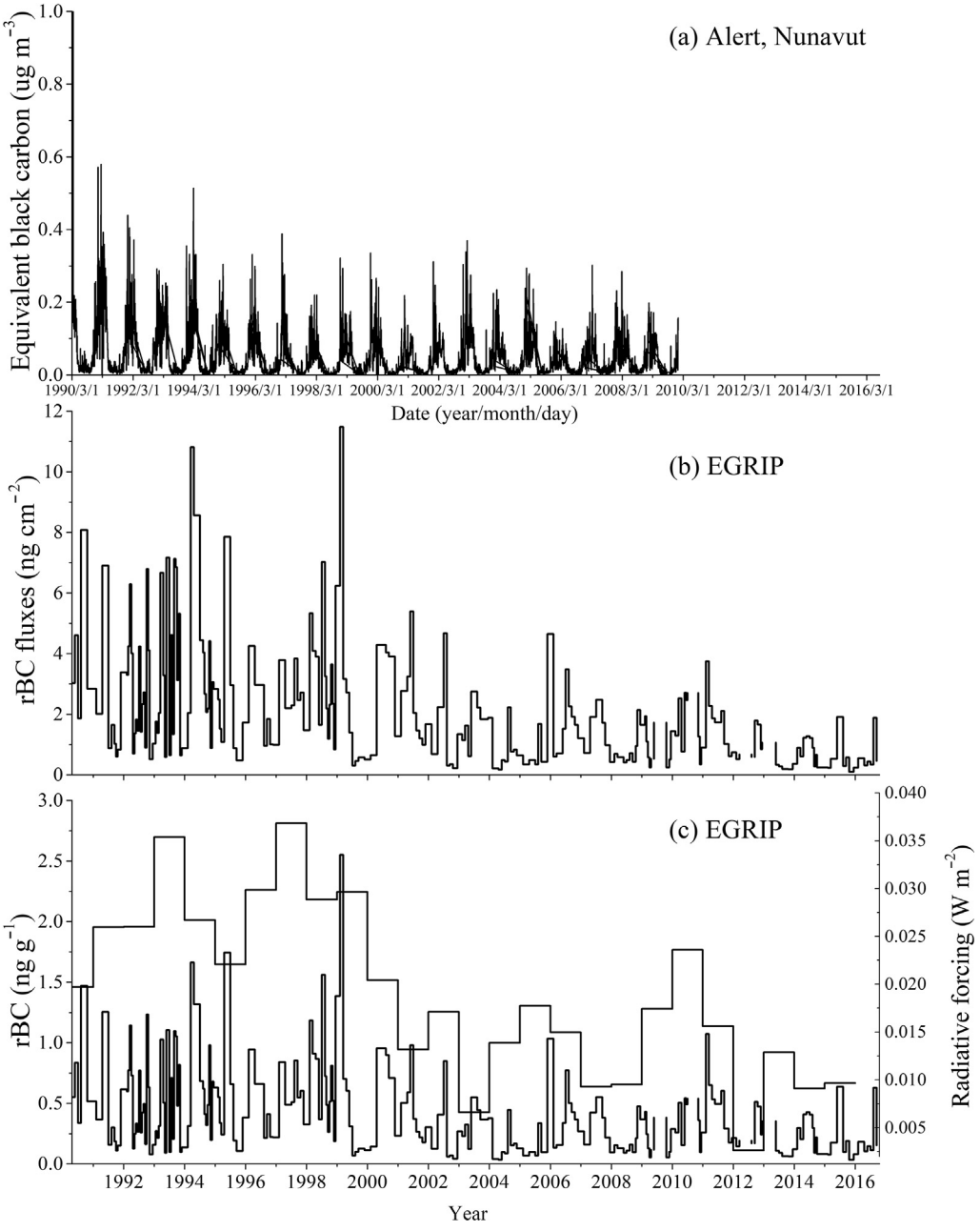

Fig. 4. Surface equivalent black carbon (EBC, absorption inferred BC) values observed at the Alert Arctic station (82.5°N, 62.3°W) (a), (b) refractory black carbon (rBC) fluxes observed in the East Greenland Ice core Project (EGRIP) shallow ice core during 1990−2016, and (c) annual mean radiative forcing and rBC concentrations observed in the EGRIP shallow ice core during 1990−2016.

thickening boundary-layer heights, as observed in the Alps (Lugauer et al., 1998; Lim et al., 2017). This result is consistent with seasonal variations in rBC recorded in the EGRIP shallow ice core. The discrepancy in BC measured values can also be attributed to the fact that the majority of emissions from biomass burning do not extend beyond 3−4 km from the source, and these emissions do not settle on the land surface, particularly in the Arctic, due to stratification in the boundary layer. This results in a disconnection in BC distribution in the atmospheric layers. It is also worth mentioning that equivalent black carbon (EBC, absorption inferred BC) values at the surface were measured using an optical technique and Aethalometer, with clear differences between the observations by the two instrument measurements as they do not measure the same thing.

An earlier study has suggested that the contribution by the Former Soviet Union (FSU) to near surface and atmospheric BC decreased by 70% and 50% from 1990 to 2009, respectively (Sharma et al., 2013). Fig. 5 shows the temporal trends in BC emissions originating from North America (Canada and the United States), Europe and China (Hoesly et al., 2018). There was a significant drop in FSU BC emissions in the early 1990s, whereas BC emissions from Europe and North America decreased steadily throughout the 1990s. Multi-model

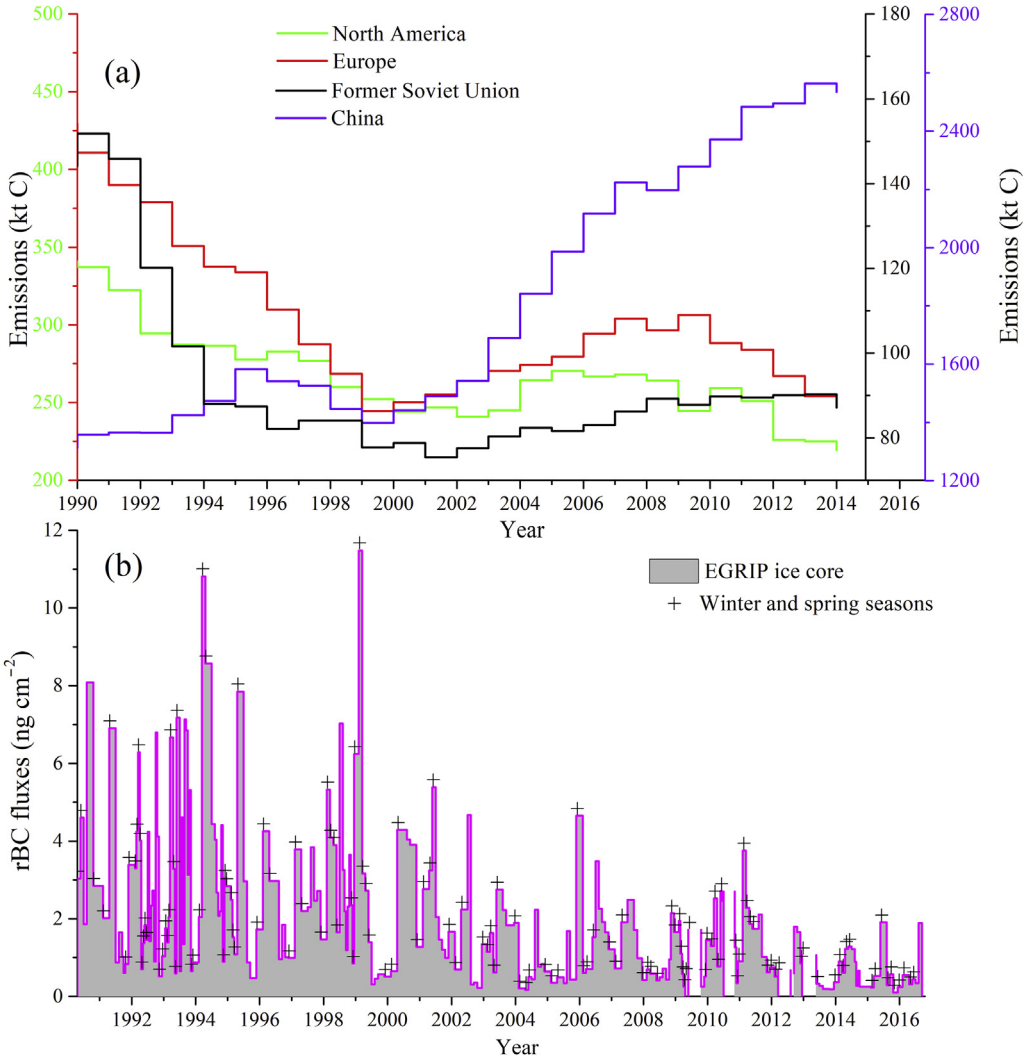

Fig. 5. Variations inBC emissions from different regions sourced from Hoesly et al. (2018) (a), and (b) rBC concentrations in the EGRIP shallow ice core during 1990–2016.

assessments of transport of pollution to the Arctic have shown that emissions from North America have the greatest influence on the deposition of BC onto the Greenland ice sheet (Shindell et al., 2008). Emissions from North America and Europe can contribute up to ~40% of total BC deposition over Greenland, with East Asia contributing ~20% (Shindell et al., 2008). An earlier study suggested that pollutants originating from South Asia contribute ~30% of total pollutant deposition in the Arctic during spring, and originate primarily from the Arctic upper troposphere/lower stratosphere (Koch and Hansen, 2005). The BC record from the EGRIP shallow ice core did not reflect the rapid increase in emissions in China since 2000. In particular, BC emissions increased rapidly in 1995 and 2003 in China. Therefore, previous models may have overestimated the contributions of BC to the high latitude of Arctic region from East Asia.

The Devon ice core (75.32° N, 81.64° W, 1750 m above sea level) shows an increasing trend in deposition of contaminants in the Arctic in the 20th century, including sulphate and lead (Pb), but not for rBC (Zdanowicz, 2017). BC records of ice cores from the Greenland NEEM and D4 sites also showed a clear drop in 1952 Common Era (C.E.) (Mcconnell et al., 2007; Zennaro et al., 2014). The rBC fluxes were calculated for the EGRIP shallow ice core to exclude emissions from fires. The declining trend in rBC concentrations during winter and spring indicated that although there have been continuous increases in BC emissions in developing countries, the intensities of these emissions have been decreasing due to improvements in technology and changes to fuel compositions at a global scale. Therefore, the records of BC in the EGRIP shallow ice core supports the assertion that the decreasing rBC in the Greenland region since 2000 can be attributed to reductions in anthropogenic emissions from North America, Europe, and the FSU. In addition, China has experienced rapid urbanization rates and other developing countries have also reduced their BC emissions. This result indicates that anthropogenic emissions of sulphate and BC are declining due to the shift in economic activity on a global scale. Therefore,

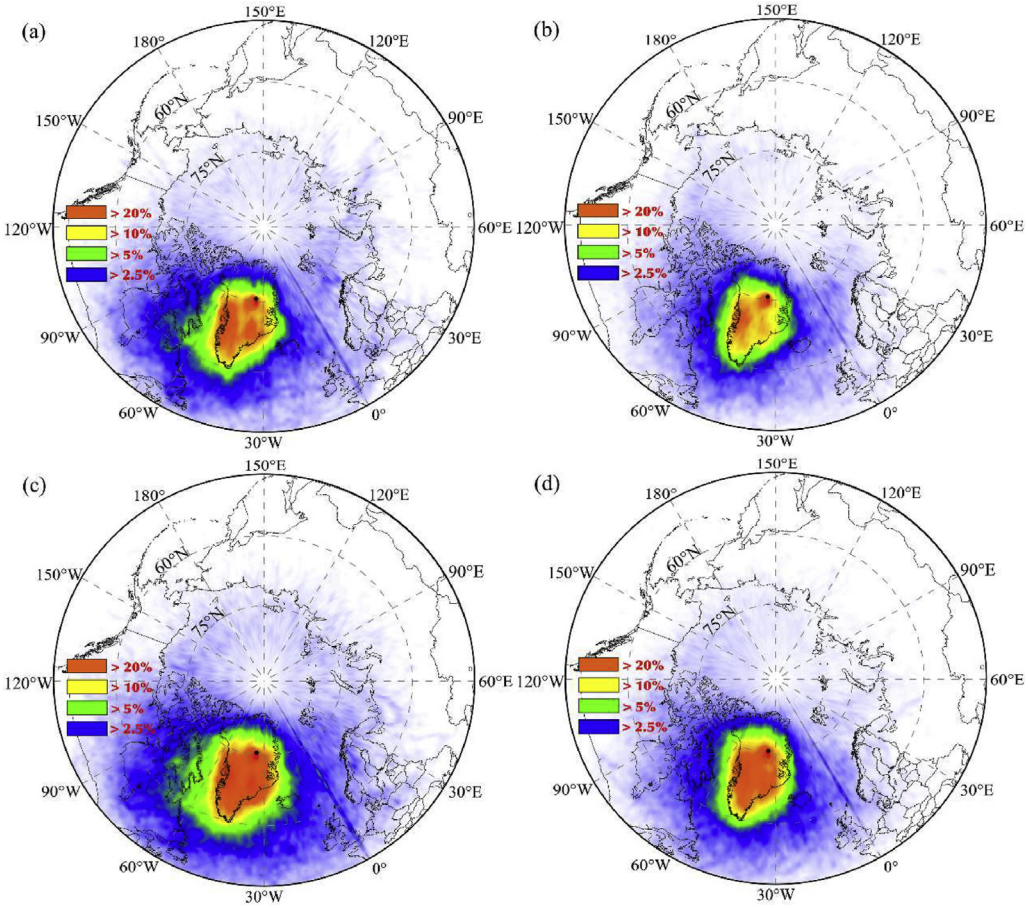

Fig. 6. Frequency plot of 7-d back trajectories during winter–spring (a and c), and summer–autumn (b and d) during 1990–2000, and 2001–2016, respectively (Backward trajectories were run at a 6-h time step. The black dot indicates the site of the East Greenland Ice core Project (EGRIP) shallow ice core. The back-trajectory data are available at the U.S. National Oceanic and Atmospheric Administration ftp://arlftp.arlhq.noaa.gov/pub/archives/reanalysis).

the variations in the rBC observed in the record of the EGRIP shallow ice core may be explained by the fact that the BC emissions from developed countries, including North America, Russia and Europe, have been decreasing.

The HYSPLIT model and the reanalysis meteorological dataset (NCEP/NCAR) were used to further determine the sources of air masses transporting BC to the EGRIP site based on the backward trajectory analysis (Draxler and Hess, 1998). The model was run at a time step of 6 h between the winter–spring and summer–autumn seasons for 1990–2000 and 2001–2016, respectively. The 7-d back trajectory frequency plotted for the EGRIP drilling site (1000 m above ground level) shows that the air mass of the winter–spring season was significantly different from that of the summer–autumn season. The winter–spring season showed considerably more air masses originating from Europe and North America (Fig. 6 a–d), with little contribution from northern regions of Russia. Since the Greenland ice sheet has experienced warming since 2000, local source of air masses have been presented for all high-level air masses over the East Greenland ice sheet (Fig. 6 c and d). These results also emphasize that the changing pattern of atmospheric circulation may be responsible for the decline in BC deposition since 2000.

4. Conclusions

The historical records of H/O isotopic ratios, ions and rBC concentrations for 1990–2016 were reconstructed from a shallow ice core taken from the East Greenland Ice core Project (EGRIP) site. Measurements of nss-SO_4^{2-} from the shallow ice core were used to identify trends in BC resulting from anthropogenic emissions. The results showed that there has been a decrease in the deposition of contaminants, including rBC and nss-SO_4^{2-} since 2000. Back trajectory analysis showed that sources of rBC deposition over East Greenland were mainly the Former USSR, Europe, and North America. Similar trends in EBC were observed at the Alert site in the Canadian Arctic, which suggests decreasing BC emissions from the burning of biomass and anthropogenic activity. There has been a declining trend in BC deposition on the East Greenland ice sheet since 2000 due to a reduction in energy-related combustion, which has resulted in a concurrent decrease in RF.

Declaration of competing interest

The authors declare no conflict of interest.

Acknowledgments

This study was supported by the Strategic Priority Research Program of the Chinese Academy of Sciences (XDA19070103), the National Key Research and Development Program of China (2018YFC1406103 and 2018YFC1406104), the National Natural Science Foundation of China (41425003), the Southern Marine Science and Engineering Guangdong Laboratory (Guangzhou) (GML2019ZD0601), the Youth Innovation Promotion Association, CAS (2020419), and the Scientific Research Foundation of the Key Laboratory of Cryospheric Sciences (SKLCSZZ-2020-09). EGRIP is organized by the Center of Ice and Climate at the Niels Bohr Institute. It is supported by funding agencies and institutions in Denmark (A.P. Møller Foundation, University of Copenhagen), the U.S. (U.S. National Science Foundation, Office of Polar Programs), Germany (Alfred Wegener Institute, Helmholtz Centre for Polar and Marine Research), Japan (National Institute of Polar Research and Artic Challenge for Sustainability), Norway (University of Bergen and Bergen Research Foundation), Switzerland (Swiss National Science Foundation), France (French Polar 270 Institute Paul−Emile Victor, Institute for Geosciences and Environmental research), and China (Chinese Academy of Sciences and Beijing Normal University).

References

Baumgardner, D., Kok, G.L., Raga, G.B., 2007. On the diurnal variability of particle properties related to light absorbing carbon in Mexico City. Atmos. Chem. Phys. 7 (1), 2517−2526. https://doi.org/10.5194/acpd-7-1623-2007.

Bisiaux, M.M., Edwards, R., Mcconnell, J.R., et al., 2012. Changes in black carbon deposition to Antarctica from two high-resolution ice core records, 1850−2000 AD. Atmos. Chem. Phys. 12 (9), 4107−4115. https://doi.org/10.5194/acp-12-4107-2012.

Dou, T., Xiao, C., Shindell, D.T., et al., 2012. The distribution of snow black carbon observed in the Arctic and compared to the GISS-PUCCINI model. Atmos. Chem. Phys. 12, 7995−8007. https://doi.org/10.5194/acp-12-7995-2012.

Draxler, R., Hess, G., 1998. An overview of the HYSPLIT_4 modeling system for trajectories, dispersion, and deposition. Aust. Meteorol. Mag. 47, 295−308.

Du, Z., Xiao, C., Ding, M., et al., 2018. Identification of multiple natural and anthropogenic sources of dust in snow from Zhongshan Station to Dome A, East Antarctica. J. Glaciol. 64 (248), 855−865. https://doi.org/10.1017/jog.2018.72.

Du, Z., Xiao, C., Mayewski, P.A., et al., 2020. The iron records and its sources during 1990–2017 from the Lambert Glacial Basin shallow ice core, East Antarctica. Chemosphere 251, 126399. https://doi.org/10.1016/j.chemosphere.2020.126399.

Flanner, M.G., Zender, C.S., Randerson, J.T., et al., 2007. Present-day climate forcing and response from black carbon in snow. J. Geophys. Res. 112, D11202. https://doi.org/10.1029/2006jd008003.

Hagler, G.S.W., Bergin, M.H., Smith, E.A., et al., 2007. Particulate and water-soluble carbon measured in recent snow at Summit, Greenland. Geophys. Res. Lett. 34 (16), 130−144. https://doi.org/10.1029/2007GL030110.

Hirdman, D., Burkhart, J.F., Sodemann, H., et al., 2010. Long-term trends of black carbon and sulphate aerosol in the Arctic: changes in atmospheric transport and source region emissions. Atmos. Chem. Phys. 10 (19), 12133−12184. https://doi.org/10.5194/acp-10-9351-2010.

Hoesly, R.M., Smith, S.J., Feng, L., et al., 2018. Historical (1750−2014) anthropogenic emissions of reactive gases and aerosols from the Community Emissions Data System (CEDS). Geosci. Model Dev. (GMD) 11 (1), 369−408. https://doi.org/10.5194/gmd-11-369-2018.

IPCC, 2013. Climate Change 2013: The Physical Science Basis. Contribution of Working Group I to the Fifth Assessment Report of the Intergovernmental Panel on Climate Change. Cambridge University Press, Cambridge and New York.

Karl, T.R., Arguez, A., Huang, B., et al., 2015. Possible artifacts of data biases in the recent global surface warming hiatus. Science 348 (6242), 1469−1472. https://doi.org/10.1126/science.aaa5632.

Kaufmann, P., Fundel, F., Fischer, H., et al., 2010. Ammonium and non-sea salt sulfate in the EPICA ice cores as indicator of biological activity in the Southern Ocean. Quat. Sci. Rev. 29 (1), 313−323. https://doi.org/10.1016/j.quascirev.2009.11.009.

Koch, D., Hansen, J., 2005. Distant origins of arctic black carbon: a goddard Institute for space studies ModelE experiment. J. Geophys. Res. 110, D04204. https://doi.org/10.1029/2004JD005296.

Koch, D., Bond, T.C., Streets, D., et al., 2007. Global impacts of aerosols from particular source regions and sectors. J. Geophys. Res. 112, D02205. https://doi.org/10.1029/2005JD007024.

Lee, Y.H., Lamarque, J.F., Flanner, M.G., et al., 2013. Erratum: evaluation of preindustrial to present-day black carbon and its albedo forcing from Atmospheric Chemistry and Climate Model Intercomparison Project (ACCMIP). Atmos. Chem. Phys. 13, 2607−2634. https://doi.org/10.5194/acp-13-6553-2013.

Legrand, M., Preunkert, S., Schock, M., et al., 2007. Major 20th century changes of carbonaceous aerosol components (EC, WinOC, DOC, HULIS, carboxylic acids, and cellulose) derived from Alpine ice cores. J. Geophys. Res. 112, D23S11. https://doi.org/10.1029/2006JD008080.

Li, C., Bosch, C., Kang, S., et al., 2016. Sources of black carbon to the Himalayan−Tibetan Plateau glaciers. Nat. Commun. 7, 12574. https://doi.org/10.1038/ncomms12574.

Li, Y., Flanner, M.G., 2018. Investigating the impact of aerosol deposition on snowmelt over the Greenland ice sheet using a large-ensemble kernel. Atmos. Chem. Phys. 18 (21), 16005−16018. https://doi.org/10.5194/acp-18-16005-2018.

Lim, S., Faïn, X., Ginot, P., et al., 2017. Black carbon variability since pre-industrial times in the eastern part of Europe reconstructed from Mt. Elbrus, Caucasus, ice cores. Atmos. Chem. Phys. 17, 3489−3505. https://doi.org/10.5194/acp-17-3489-2017.

Lin, G., Penner, J.E., Flanner, M.G., et al., 2014. Radiative forcing of organic aerosol in the atmosphere and on snow: effects of soa and brown carbon. J. Geophys. Res. 119 (12), 7453−7476. https://doi.org/10.1002/2013JD021186.

Lugauer, M., Baltensperger, U., Furger, M., et al., 1998. Aerosol transport to the high Alpine sites Jungfraujoch (3454 m asl) and Colle Gnifetti (4452 m asl). Tellus B 50 (1), 76−92. https://doi.org/10.3402/tellusb.v50i1.16026.

Mcconnell, J.R., Edwards, R., Kok, G.L., et al., 2007. 20th-century industrial black carbon emissions altered Arctic climate forcing. Science 317, 1381−1384. https://doi.org/10.1126/science.1144856.

Ming, J., Xiao, C., Cachier, H., et al., 2009. Black carbon (BC) in the snow of glaciers in west China and its potential effects on albedos. Atmos. Res. 92 (1), 114−123. https://doi.org/10.1016/j.atmosres.2008.09.007.

Mori, T., Goto-Azuma, K., Kondo, Y., et al., 2019. Black carbon and inorganic aerosols in Arctic snowpack. J. Geophys. Res. 124 (23) https://doi.org/10.1029/2019JD030623.

Mouteva, G.O., Czimczik, C.I., Fahrni, S.M., et al., 2015. Black carbon aerosol dynamics and isotopic composition in Alaska linked with boreal fire emissions and depth of burn in organic soils. Global Biogeochem. Cycles 29 (11), 1977−2000. https://doi.org/10.1002/2015GB005247.

Osmont, D., Wendl, I.A., Schmidely, L., et al., 2018. An 800 year high-resolution black carbon ice-core record from Lomonosovfonna. Svalbard. Atmos. Chem. Phys. 18, 12777−12795. https://doi.org/10.5194/acp-18-12777-2018.

Paris, J.D., Stohl, A., Nédélec, P., et al., 2009. Wildfire smoke in the Siberian Arctic in summer: source characterization and plume evolution from airborne measurements. Atmos. Chem. Phys. 9 (23), 9315−9327. https://doi.org/10.5194/acpd-9-18201-2009.

Parkinson, C.L., Comiso, J.C., 2013. On the 2012 record low Arctic sea ice cover: combined impact of preconditioning and an August storm. Geophys. Res. Lett. 40, 1356−1361. https://doi.org/10.1002/grl.50349.

Polashenski, C.M., Dibb, J.E., Flanner, M.G., et al., 2015. Neither dust nor black carbon causing apparent albedo decline in Greenland's dry snow zone: implications for MODIS C5 surface reflectance. Geophys. Res. Lett. 42, 9319−9327. https://doi.org/10.1002/2015GL065912, 2015.

Ruppel, M.M., Isaksson, I., Ström, J., et al., 2014. Increase in elemental carbon values between 1970 and 2004 observed in a 300-year ice core from Holtedahlfonna (Svalbard). Atmos. Chem. Phys. 14 (20), 11447−11460. https://doi.org/10.5194/acp-14-11447-2014.

Schneidemesser, E.V., Schauer, J.J., Hagler, G.S.W., et al., 2009. Concentrations and sources of carbonaceous aerosol in the atmosphere of Summit, Greenland. Atmos. Environ. 43 (27), 4155−4162. https://doi.org/10.1016/j.atmosenv.2009.05.043.

Schwarz, J.P., Gao, R.S., Fahey, D.W., et al., 2006. Single-particle measurements of midlatitude black carbon and light-scattering aerosols from the boundary layer to the lower stratosphere. J. Geophys. Res. 111, D16207. https://doi.org/10.1029/2006JD007076.

Schwarz, J.P., Spackman, J.R., Gao, R.S., et al., 2010. Global-scale black carbon profiles observed in the remote atmosphere and compared to models. Geophys. Res. Lett. 37 (18) https://doi.org/10.1029/2010GL044372.

Sharma, S., Ishizawa, M., Chan, D., et al., 2013. 16-year simulation of Arctic black carbon: transport, source contribution, and sensitivity analysis on deposition. J. Geophys. Res. 118 (2), 943−964. https://doi.org/10.1029/2012JD017774.

Shindell, D.T., Chin, M., Dentener, F., et al., 2008. A multi-model assessment of pollution transport to the Arctic. Atmos. Chem. Phys. 8, 5353−5372. https://doi.org/10.5194/acp-8-5353-2008.

Sigl, M., Abram, N.J., Gabrieli, J., et al., 2018. 19th century glacier retreat in the Alps preceded the emergence of industrial black carbon deposition on high-alpine glaciers. Cryosphere 12 (10), 3311−3331. https://doi.org/10.5194/tc-12-3311-2018.

Skiles, S.M., Flanner, M., Cook, J.M., et al., 2018. Radiative forcing by light-absorbing particles in snow. Nat. Clim. Change 8, 964−971. https://doi.org/10.1038/s41558-018-0296-5.

Steen-Larsen, H.C., Masson-Delmotte, V., Sjolte, J., et al., 2011. Understanding the climatic signal in the water stable isotope records from the NEEM shallow firn/ice cores in northwest Greenland. J. Geophys. Res. 116, D06108. https://doi.org/10.1029/2010JD014311.

Stephens, M., Turner, N., Sandberg, J., 2003. Particle identification by laser-induced incandescence in a solid-state laser cavity. Appl. Optic. 42 (19), 3726−3736. https://doi.org/10.1364/AO.42.003726.

Stohl, A., 2006. Characteristics of atmospheric transport into the Arctic troposphere. J. Geophys. Res. 111, D11306. https://doi.org/10.1029/2005jd006888.

Stohl, A., Klimont, Z., Eckhardt, S., et al., 2013. Black carbon in the Arctic: the underestimated role of gas flaring and residential combustion emissions. Atmos. Chem. Phys. 13 (17), 8833−8855. https://doi.org/10.5194/acp-13-8833-2013.

Thevenon, F., Anselmetti, F.S., Bernasconi, S.M., et al., 2009. Mineral dust and elemental black carbon records from an Alpine ice core (Colle Gnifetti glacier) over the last millennium. J. Geophys. Res. Atmos. 114 (D17) https://doi.org/10.1029/2008JD011490.

Vallelonga, P., Christianson, K., Alley, R.B., et al., 2014. Initial results from geophysical surveys and shallow coring of the Northeast Greenland Ice Stream (NEGIS). Cryosphere 8, 1275−1287. https://doi.org/10.5194/tc-8-1275-2014.

Wang, M., Xu, B., Kaspari, S.D., et al., 2015. Century-long record of black carbon in an ice core from the Eastern Pamirs: estimated contributions from biomass burning. Atmos. Environ. 115, 79−88. https://doi.org/10.1016/j.atmosenv.2015.05.034.

Warneke, C., Bahreini, R., Brioude, J., et al., 2009. Biomass burning in siberia and Kazakhstan as an important source for haze over the Alaskan arctic in April 2008. Geophys. Res. Lett. 36 (2) https://doi.org/10.1029/2008GL036194.

Warren, S.G., 2019. Light-absorbing impurities in snow: a personal and historical account. Front. Earth Sci. 6, 250. https://doi.org/10.3389/feart.2018.00250.

Winiger, P., Barrett, T.E., Sheesley, R.J., et al., 2019. Source apportionment of circum-arctic atmospheric black carbon from isotopes and modeling. Sci. Adv. 5 (2) https://doi.org/10.1126/sciadv.aau8052.

Xu, B., Cao, J., Hansen, J., et al., 2009. Black soot and the survival of Tibetan glaciers. Proc. Natl. Acad. Sci. U.S.A. 106 (52), 22114−22118. https://doi.org/10.1073/pnas.0910444106.

Zdanowicz, C.M., Proemse, B.C., Edwards, R., et al., 2018. Historical black carbon deposition in the Canadian High Arctic: a >250-year long ice-core record from Devon Island. Atmos. Chem. Phys 18, 12345−12361. https://doi.org/10.5194/acp-18-12345-2018, 2018.

Zennaro, P., Kehrwald, N., McConnell, J.R., et al., 2014. Fire in ice: two millennia of boreal forest fire history from the Greenland NEEM ice core. Clim. Past 10, 1905−1924. https://doi.org/10.5194/cp-10-1905-2014.